

December 1982

# **Reliability Aspects of a Floating Gate E<sup>2</sup>PROM**

**Bruce Euzent, Nick Boruta,  
Jimmy Lee and Ching Jenq**  
Intel Corporation

Based on presentation at 1981 International Reliability Physics Symposium, Orlando, Florida, April 7, 1981.

©Intel Corporation, 1982.

## INTRODUCTION

Electrically Erasable Programmable Read Only Memories ( $E^2$ PROMs) that can be electrically erased and written one byte at a time are new components being used in computer systems. The  $E^2$ PROM is particularly attractive in applications requiring field update of program store memory or non-volatile data capture. It is only recently that  $E^2$ PROMs which operate via Fowler-Nordheim tunneling to a floating polysilicon gate have become available. The  $E^2$ PROM has the data retention requirements of earlier generations of PROMs, but also must maintain its field-programmable characteristics over its device life.

In this paper we shall first review the basic operation of the Intel 2816  $E^2$ PROM cell. Intrinsic failure mechanisms which limit the applications of  $E^2$ PROMs will be examined, and then defect mechanisms will be discussed. Finally lifetest data will be presented to predict operating failure rates.

## Device Operation

The Intel 2816 uses the FLOTOX structure, which has been discussed in detail in previous literature<sup>1</sup>. Basically, it utilizes an oxide of less than 200Å thick between the floating polysilicon gate and the N+ region as shown in Figure 1.

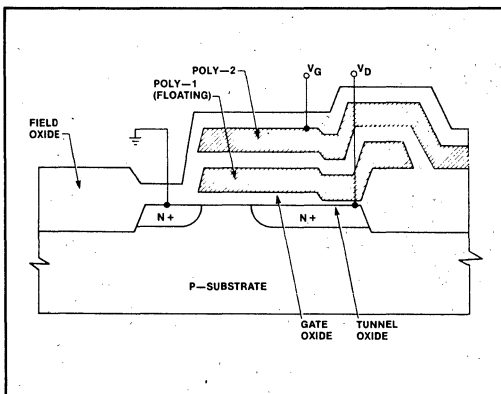


Figure 1. FLOTOX Device Structure Cross Section

Both erase and write are accomplished by tunneling the electrons through thin oxide using the Fowler-Nordheim mechanism<sup>2</sup>. The I-V characteristic of Fowler-Nordheim tunneling is shown in Figure 2, where the current is approximately exponentially dependent on the electric field applied to the oxide.

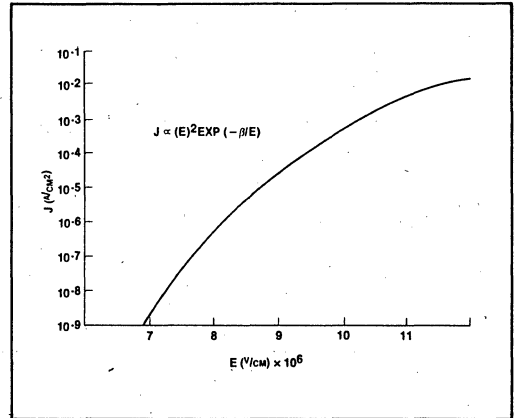


Figure 2. Fowler-Nordheim Tunneling I-V Characteristic

During the erase operation, approximately 20V is applied to the top gate of each cell in the byte while the drain is kept at ground potential. The electrical field in the thin oxide region is directed from the floating gate to the N+ region such that electrons tunnel through the oxide and are stored on the floating gate. This shifts the cell threshold in the positive direction causing the cell to shut off current flow and present a logical "1" at its output (as seen in Figure 3a).

On the other hand, when the cell is written to logic "0", the top gate is pulled down to ground potential and a high voltage is applied to the drain (with the source end floating). Electrons are depleted from the floating gate

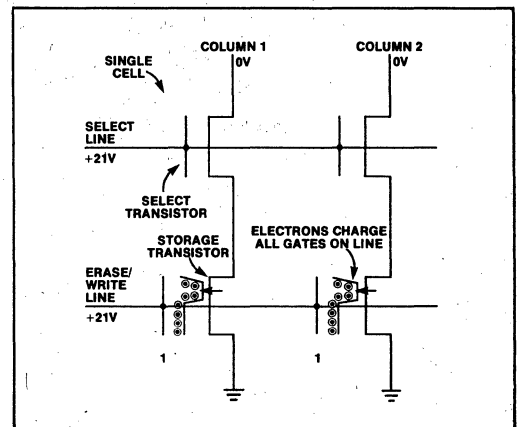


Figure 3a. Schematic of Memory Cell Operation During Erase

as seen in Figure 3b, and the cell is left with a negative threshold. Since the interpoly oxide is much thicker than the "tunnel oxide" and the electric field across the interpoly oxide is much smaller, the erase and write operations are predominantly controlled by the thin oxide region.

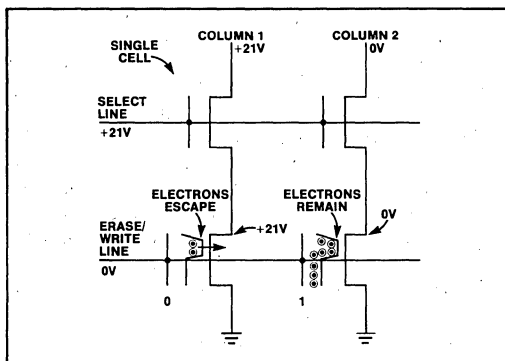


Figure 3b. Schematic of Memory Cell Operation During Write

## Read Retention

The floating gate structure is known for its excellent charge retention properties. The reliability of this structure in the case of the EPROM device has been reported before<sup>3</sup>. The only remaining concern of the data retentivity of the 2816 is possible charge gain or loss through the tunnel oxide due to Fowler-Nordheim tunneling. The maximum electric field is built up across the tunnel oxide for a written cell, one that has a net positive charge on the floating gate. In this state the positive top gate voltage creates an electric field which adds to the field created by the positive charge on the floating gate, and there exists the probability that electrons may tunnel to the floating gate and shift the cell threshold. The band diagram of this condition is shown in Figure 4. However, the amount of current which may pass through the thin oxide during read or deselect is kept low by biasing the top gate of the memory cell at an internally generated voltage less than  $V_{CC}$ . The effect on the threshold shift of the cell can only be observed after long-term stress. Under this condition, the accelerated voltage test can be very useful.

If we assume Fowler-Nordheim tunneling is the predominant mechanism governing the movement of electrons, the threshold shift of the cell will be dependent solely on the voltage between the top gate and the  $N^+$  region. This has been proven to be true in both simulations and experiments, where we found that

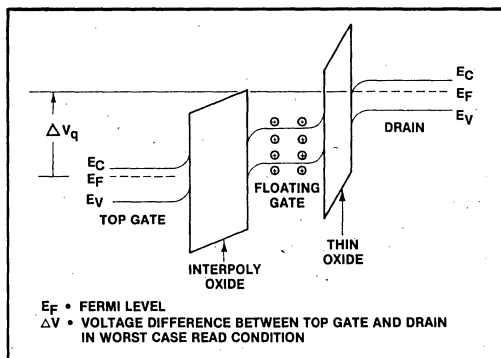


Figure 4. Band Diagram During Read of Written Cell

there is a one-to-one relationship between the  $V_T$  and the stress voltage. In other words, we can stress the device by applying a higher voltage to the top gate such that the change of the threshold voltage can be measured. The data then will be used to predict the same characteristics at the much lower normal read voltage. In Figure 5, the aforementioned simulation and experimental data are shown. The cell was biased at a voltage 4V higher than the normal read condition and the threshold voltage of the cell was monitored over a period of a week. A simulation was also generated to compare with the observed threshold shift and to demonstrate the technique we use to predict whether the data retention of the cell is accurate. As can be seen in the Figure 4, even under the accelerated voltage test the cell  $V_T$  still will not cross above the sense level after more than 10 years. Similar data has also been taken by writing the cell to a more negative initial threshold. In this case, the shift of the threshold can be observed at a stress of normal read voltage. Clearly, a 1V/1V relationship holds and an extrapolation can be made that the correct data will be retained for more than 10 years of continuous read.

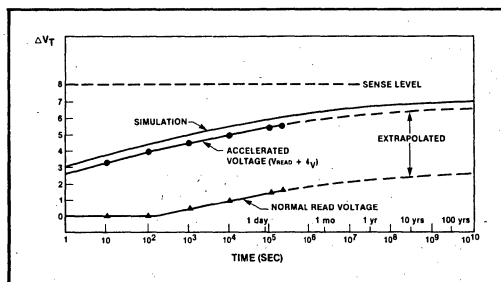
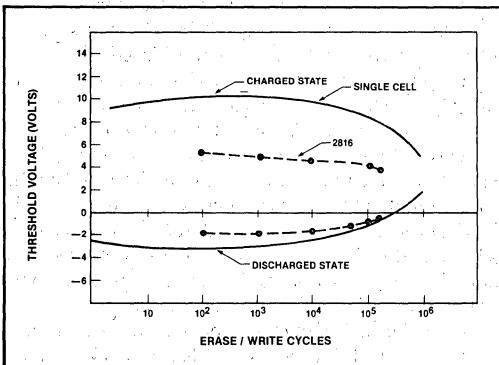


Figure 5. Single Cell Threshold Voltage Shift vs. Log Time During Read of a Written Cell

## Intrinsic Charge Trapping

An ideal feature of a tunneling dielectric is that it should never remember the number of electrons that passed through it or the voltage that was previously applied across the film. Unfortunately, for thermally grown  $\text{SiO}_2$  there always exists a certain number of electron and hole traps<sup>4-9</sup>. When these traps are occupied the net charging state of the tunnel oxide will be changed and thus cause the tunneling current across the film to vary if the applied voltage has remained the same.

Figure 6 plots the threshold voltage of a 2816 cell in erase (charged) and write (discharged) states as a function of erase/write cycles. The solid line is for a single cell, while the dashed line is for a typical 2816 array. It is seen that the threshold window, defined as the difference between the erase and write threshold, is slightly increased in the first few E/W cycles and then saturates and remains almost constant until  $10^4$  cycles. From that point, the window begins to narrow gradually until around  $10^6$  cycles where the window is collapsed.



**Figure 6. Typical Cell and Device Window vs. Log Cycles**

Our study shows that the behavior of the widening and narrowing of the threshold window can be explained by charge trapping in tunnel oxide. The window widening effect is found to be caused by the following mechanism:

Assume a cell is to be erased following a write cycle. During the preceding write cycle, the floating gate is biased negatively relative to the substrate. A layer of positive charge will be formed, either through the tunneling of holes from Si into  $\text{SiO}_2$  or electrons in the reverse direction. These positive charges are in general at 20–30 Å away from the  $\text{SiO}_2/\text{Si}$  interface, as in Figure 7a. At the beginning of the erase step, the positive

charges will cause an increase in electric field at the injection interface, i.e.,  $\text{SiO}_2/\text{Si}$  interface, as shown in Figure 7b. This will in turn increase the tunneling current to the floating gate, where the amount of stored electrons is thus increased, causing the erase threshold to increase. During the erase cycle, however, the polarity of bias voltage across the tunnel oxide will cause the positive charge at  $\text{SiO}_2/\text{Si}$  interface to be neutralized through the reverse tunneling mechanism that forms these charges. At the same time a new layer of positive charges is formed near the anode<sup>11, 12</sup>, i.e., poly/ $\text{SiO}_2$  interface, as shown in Figure 7c. These charges will then cause the write threshold to increase through the same mechanism as that discussed for the erase threshold. In addition to positive charge trapping, our study also shows that there is a uniform distribution of electron traps throughout the oxide<sup>11, 12</sup>. When the cell is erased or written, electrons are injected through the oxide and some of them will be captured by these traps,

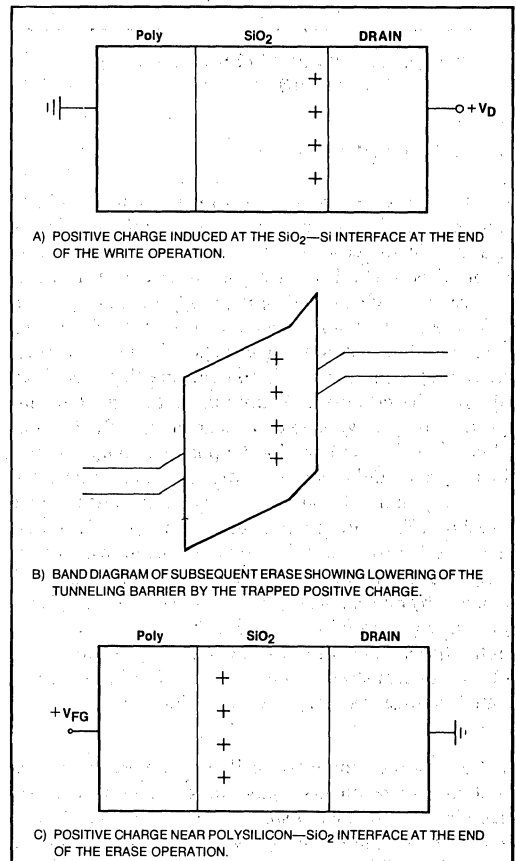


**Figure 7. Threshold Window Widening**

causing the build-up of negative charges in the oxide, as shown in Figure 8. The negative charges will reduce the electric field at the injection interface, thus decreasing the tunneling current and causing the threshold window to narrow. It has been found that the electron traps are not only preexisting in the oxide but also generated during the E/W cycles<sup>9-12</sup> because of the high field stress and the accompanying high current flow. The non-saturated build-up of negative charges, because of the continuous generation of electrons traps will finally cause the threshold window to collapse.

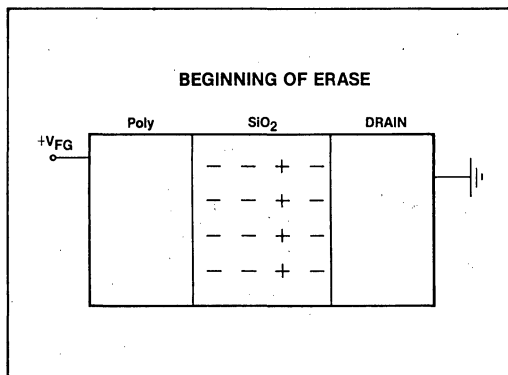


Figure 8. Negative Charges Trapped Uniformly Across Tunnel Oxide

## Defect Charge Loss

EPROMs have been shown to have excellent data retention<sup>3</sup>. In this section we will discuss data retention studies that have been performed on the Intel 2816 E<sup>2</sup>PROM. Since in E<sup>2</sup>PROMs the number of Erase/Write cycles during the device lifetime is 3 to 4 orders of magnitude greater than in the EPROM, we will also need to address the effects of cycling on data retention.

As in the case of EPROMs the charge loss from the floating gate can be described as either intrinsic or defect-related. We will discuss the defect-related charge loss since the intrinsic charge loss on a typical device is identical to the EPROM and has been described before<sup>3</sup>.

Analysis of cells exhibiting defect-related charge loss shows that the leakage current has an exponential dependence on the potential of the floating gate. This is different from the EPROM where defect leakage current exhibits a linear (ohmic) dependence on voltage.<sup>3</sup> The exponential dependence is indicative of electron tunneling. The effect of the defect, then, is the lowering or narrowing of the thin oxide barrier, allowing tunnel-

ing to occur at voltage differences between the floating gate and the drain that would ordinarily be insufficient to support tunneling.

Erase/write cycling effects on data retention were studied by comparing 250°C retention before cycling to that after 10,000 cycles. Figure 9 shows a plot of the cumulative % data retention failure during 500 hours 250°C retention bake. Data from the Intel 2716 EPROM is included as a comparison. From this data it is clear that the retention failure rate closely resembles that of the Intel 2716 EPROM.

Since the defect charge loss failure mechanism is temperature activated it is simple to construct screens on a production basis for these types of failures similar to those used on EPROMs.

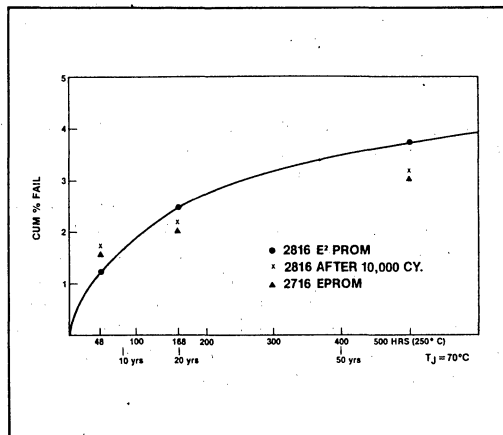


Figure 9. Intel 2816 Data Retention at 250°C, Percent Fail vs. Time

## Accelerated Test Results

An E<sup>2</sup>PROM has an additional reliability requirement over standard PROMs. Besides the integrity of data retention, an E<sup>2</sup>PROM must withstand up to 10,000 erase and write programming pulses per byte. Besides the previously discussed window closing phenomenon there are reliability considerations due to high voltage operation. Dielectric breakdown<sup>13</sup> is a common MOS failure mechanism, which has been shown to be highly voltage accelerated. The reliability of the Intel 2816 during erase/write cycles was measured by performing the full number of erase/write cycles on each byte. Erase/write cycling was done at 70°C and 25°C with no difference in observed failure rate between these temperatures.

The results of erase/write cycling are shown in Figure 10A. The devices under test are completely tested after 2,000, 5,000 and 10,000 total cycles on each byte. The devices are programmed to several data patterns and tested to data sheet specifications. In addition, the devices are tested for high temperature data retention. As can be seen from Figure 10A, the failure rate per 1000 cycles decreases as a function of the number of cycles, which is typical for defect mechanisms such as dielectric breakdown.<sup>13</sup> From the time the initial data was gathered in 1981, recent data (Figure 10A) has shown the failure rate to have been reduced by a factor of 2.

Two major types of failures were found: Tunnel oxide breakdown and oxide breakdown in the row select circuitry. These failures were minimized by using standard screening techniques for oxide breakdown. Figure 10B shows the failure mode distribution found during erase/write cycling of 549 devices.

Tunneling oxide breakdown failures are cells which fail either to program or to retain data following programming due to conduction through the thin oxide at low electric fields. In the case of the programming failures, the breakdown extends all the way through the oxide layer. The data retention failures exhibit characteristics similar to those of the defect charge loss failures discussed in the previous section and are probably due to a partially broken down oxide layer. Further cycling of this type of retention failure has been found to result in it becoming a programming failure.

Table I shows expected failure rates in %/1000 hours at a 60% upper confidence level based on expected device life and the average number of cycles per byte. In a typical system it is expected that some bytes will be written more often than others, so these failure rates serve as a guideline.

As can be seen in Table II, acceptable failure rates are achieved for the design goal of 10,000 erase/write cycles per byte. To achieve 10,000 cycles per byte in ten (10) years, each byte must be altered approximately three times per day.

As a final verification of device reliability a standard high temperature lifetest at 125°C was performed on devices programmed with a checkerboard data pattern. The lifetest was performed on devices with no additional cycles and devices with 10,000 cycles on each

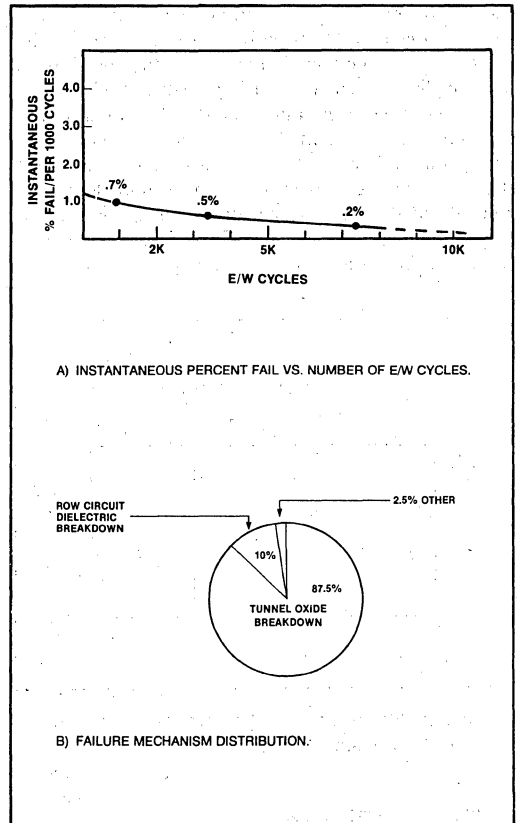


Figure 10. Erase/Write Cycling Results

Table I. Erase/Write Cycling Failure Rate (per 1000 hours at a 60% UCL)

Device Life	No. of Cycles		
	2000	5000	10,000
5 years	.035	.06	.092
10 years	.017	.029	.047
20 years	.009	.017	.023

Table II. 125°C Lifetest Results

Cycles	48 Hrs	168 Hrs	500 Hrs	1000 Hrs	2000 Hrs
0	0/1422	1/1422 <sup>a</sup>	1/443 <sup>b</sup>	0/429	0/270
10,000	0/336	0/336	0/336	0/150	—
Total	0/1758	1/1758	1/779	0/579	0/270

Failure Analysis:  
a) = Non-repeatable charge gain, contamination, lev.  
b) = Input leakage, contamination, lev.

byte. As can be seen from the data in Table II standard MOS failure mechanisms were observed. This data is significant in that it shows no additional defect mechanisms related to data retention or erase/write cycling of the Intel 2816 E<sup>2</sup>PROM.

Failure rate predictions are made in Table III at a 60% upper confidence level for both 55°C and 70°C operation. The .013%/1000 hrs. failure rate at 55°C shows good reliability comparable to other semiconductor memories.

Table III. Failure Rate Predictions at a 60% U.C.L.

125°C Device Hrs.	Activation Energy	Equivalent Hours		Lifetest Failures	Failure Rate % per 1000 Hrs.	
		55°	70°		55°C	70°
3.2x10 <sup>6</sup>	0.3 eV	2.1x10 <sup>7</sup>	1.3x10 <sup>7</sup>	0	.004	.007
3.2x10 <sup>6</sup>	0.6 eV	1.3x10 <sup>8</sup>	5.3x10 <sup>7</sup>	0	.001	.002
3.2x10 <sup>6</sup>	1.0 eV	1.6x10 <sup>9</sup>	3.4x10 <sup>8</sup>	2	.000	.001
				Combined	.005	.010

## SUMMARY

This paper has discussed a number of E<sup>2</sup>PROM failure mechanisms for both erase/write cycling and data retention. It has been shown that Fowler-Nordheim tunneling used for programming does not affect data retention. Erase/write cycling has been shown to degrade device margins by only a small amount and is easily guardbanded. Erase/write cycling does contribute to a significant portion of the observed failure rate due to oxide breakdown under high field operation. Finally, it has been shown that E<sup>2</sup>PROMs can perform reliably in applications requiring up to 10,000 erase/write cycles per byte.

## REFERENCES

1. W. S. Johnson, et al, "16-K EE-PROM Relies on Tunneling for Byte-Eraseable Program Storage," *Electronics*, February 28, 1980, p. 113-117.
2. R. Williams, *Phys. Rev.*, Vol. 140, p. 569, 1965.
3. R. E. Shiner, J. M. Caywood, B. L. Euzent, "Data Retention in EPROMs," 1980 Proceedings of the 18th Annual Reliability Physics Symposium, p. 238-243.
4. E. H. Nicolian, C. N. Berglund, P. F. Schmidt, I. M. Andrews, *J. Appl. Phys.*, Vol. 42, p. 5654, 1971.
5. M. H. Woods and R. Williams, *J. Appl. Phys.*, p 47, 1082, 1976.
6. W. C. Johnson, *IEEE Trans. Nucl. Sci.*, p. NS-22, 2144, 1975.
7. D. J. DiMaria, Proceeding of the International Topical Conference on the Physics of SiO<sub>2</sub> and its Interfaces, p. 160, 3/78.
8. E. Harari, *Appl. Phys. Letter*, p. 30, 601, 1977.
9. C. S. Jenq, "High Field Generation of Interface States and Electron Traps in MOS Capacitors," Ph.D. dissertation, Princeton Univ., 12/77.
10. C. S. Jenq, W. C. Johnson, "High Field Generation of Electron Traps in MOS Capacitors," presented in Semiconductor Interface Specialist Conference, 12/77.
11. C. S. Jenq, T. R. Rangarath, C. H. Huang, "Charge Trapping in Floating Gate Tunnel Oxide" presented in 1980 Non-Volatile Semiconductor Memory workshop to be published.
12. D. R. Young, "Electron Trapping in SiO<sub>2</sub>", presented in 1980 Non-Volatile Semiconductor Memory workshop.
13. D. Crook, "Method of Determining Reliability Screen for Time Dependent Dielectric Breakdown," 1979 17th Annual Reliability Physics Symposium Proceedings, p. 1-5.